http://www.aimspress.com/journal/mine

Mathematics in Engineering, 3(2): 1–21.
DOI:10.3934/mine.2021016
Received: 16 March 2020
Accepted: 28 May 2020
Published: 29 June 2020

Research article

Beams with an intermediate pier: Spectral properties, asymmetry and stability†

Maurizio Garrione*

Dipartimento di Matematica, Politecnico di Milano, Piazza Leonardo da Vinci, 32 - 20133 Milano, Italy

† **This contribution is part of the Special Issue:** Qualitative Analysis and Spectral Theory for Partial Differential Equations
Guest Editor: Veronica Felli
Link: www.aimspress.com/mine/article/5511/special-articles

* **Correspondence:** Email: maurizio.garrione@polimi.it.

Abstract: We deal with beams with an intermediate pier, motivated by the investigation of the stability of suspension bridges with two spans. First, we provide a complete spectral theorem for the associated linear stationary fourth-order problem with hinged boundary conditions, determining the eigenvalues and discussing their optimality (in a suitable sense) in terms of the position of the pier. Then, we consider a related nonlinear model with a restoring force of superquadratic displacement type, discussing its stability both from a linear and from a suitable nonlinear point of view. We determine the position of the pier maximizing the stability of the structure and we compare the energy thresholds of instability under hinged, clamped or mixed (left-clamped and right-hinged) boundary conditions. In any case, we highlight that an asymmetric structure is in general more stable.

Keywords: multi-point ODEs; beams; intermediate pier; asymmetry; stability; optimal position

1. Introduction

In this paper, we deal with a beam – represented by a segment $[\alpha,\beta]$ - divided into two adjacent spans by a fixed internal point $\sigma \in (\alpha,\beta)$, and we study some evolution models for its (downward) vertical displacement $u(x,t)$, for $x \in (\alpha,\beta)$ and $t > 0$. In correspondence of $x = \alpha$, $x = \beta$ and $x = \sigma$, we always assume the null displacement condition $u = 0$. We devote special attention to the linear spectral theory for the associated stationary problem and to the (linear and nonlinear) stability for the evolution models, in dependence on the position of the internal constraint.

The study of the stability for fourth-order (ODE and) PDE models has a significant motivation in the attempt of explaining completely, from a mathematical point of view, the events leading to the famous collapse of the Tacoma Narrows Bridge in 1940. The fourth-order term therein comes from the bending energy of the structure and makes the study not at all trivial. Usually one produces a linear stationary theory providing a suitable basis of eigenfunctions, which are used to implement a Galerkin procedure; after neglecting the high modes, corresponding to high spatial frequencies and so to unrealistically large energies, the object of interest is the finite-dimensional system of ODEs describing the dynamics of the first N Fourier components of the solution, for a suitable positive integer N.

The main feature of the beams considered in this paper is the presence of an internal pier, namely an intermediate point where the displacement is forced to be zero, mimicking the presence of an intermediate pylon in a real structure (for a real bridge with rectangular shape, we are meaning a couple of pylons, placed at the same distance from the endpoints on each of the long edges). While in absence of such a constraint the linear theory becomes trivial, here the problem has to be framed in a proper variational setting taking into account the "multi-point" conditions and the regularity of the solutions is in general lost. For this reason, standard results of Sturm-Liouville type for the determination of the eigenfunctions seem difficult to be applied and we thus start producing a spectral theorem for the stationary eigenvalue problem. This was done in [5] for a hinged beam with two symmetric piers; as shown in Section 2, from the very beginning one may take advantage of the material developed therein after a suitable rescaling, but we prefer to proceed directly. In Theorem 1, we explicitly determine the eigenvalues λ and the eigenfunctions e_λ in dependence on σ; it turns out that the eigenvalues can be organized into a sequence of "well separated" smooth curves $\sigma \mapsto \lambda(\sigma)$ in the (σ, λ)-plane (Proposition 3 and Theorem 7). Among the eigenfunctions, two classes turn to be relevant: the regular (C^4 and thus C^∞) ones and the ones which possess a double zero in the pier. Their relevance lies in the fact that the associated eigenvalues respectively correspond to local maxima and local minima on the eigenvalue curves, as shown in Theorem 5. This seems to be a general fact that can be extended to problems with an arbitrary number of internal constraints, even if the way we prove it is by direct computation.

We then turn to the study of the nonlinear evolution equation

$$u_{tt} + u_{xxxx} + \|u\|_{L^2}^2 u = 0, \qquad x \in [\alpha, \beta],\ t > 0, \tag{1.1}$$

where the restoring force is given by a superquadratic displacement-type nonlinearity. The reasons for the choice of such a nonlinear term were explained in [4]; besides allowing a quite precise theoretical analysis of the model (see, e.g., [2]), it seems to be more in line with the behavior observed in real bridges, see [4, Section 3.6]. We are here concerned with stability, meant both in the usual linear sense and according to a more applied definition given in [3], with a twofold purpose: to investigate, in terms of stability, the optimal position of the pier and the optimal boundary conditions among hinged ($u_{xx} = 0$), clamped ($u_x = 0$) or mixed (left-clamped and right-hinged: $u_x(\alpha, t) \equiv 0$, $u_{xx}(\beta, t) \equiv 0$). Such an analysis will be performed for bi-modal solutions – i.e., solutions of the form $u(x, t) = w(t)e_\lambda(x) + z(t)e_\rho(x)$, with e_λ and e_ρ denoting two distinct eigenfunctions of the stationary eigenvalue problem – according to the following scheme. For fixed σ, we define an energy threshold of instability $E_{\lambda,\rho}(\sigma)$ for each couple of eigenvalues (λ, ρ). Selecting a finite number of modes N and repeating the analysis for all the related $N(N-1)/2$ couples, the energy threshold of instability of the beam with a pier at σ will be defined as the minimum of $E_{\lambda,\rho}(\sigma)$ among all possible choices of the couple (λ, ρ); for smaller

values of the energy, such a beam is stable. The optimal position of the pier is then the one maximizing $\sigma \mapsto \min_{\lambda,\rho} E_{\lambda,\rho}(\sigma)$. For the linear stability, the classical theoretical framework (see, e.g., [12]) works well in this setting, through a technique similar to the one used in [4]: We linearize the 2×2 ODE system in the unknowns w, z around the solution which has null z-component and we investigate whether the trivial solution $z \equiv 0$ is stable for the resulting equation in the z-variable. Using some classical criteria like the Burdina one [1, 4, 6], together with the results in [8, 9], we are able to determine sharply the regions of instability as functions of $w(0)/\lambda^2$ and ρ^4/λ^4, and hence each value $E_{\lambda,\rho}(\sigma)$ is explicit. The nonlinear stability analysis, which is performed through numerical simulations, is instead explained in Section 3. The results of the two investigations agree (as also observed in [4]) and suggest that

the optimal position of the pier is approximately the one for which the longer span is twice as long as the shorter one

and

the optimal boundary conditions in terms of stability are the clamped ones.

In particular, the choice $\sigma = (\alpha + \beta)/2$, dividing the beam into two spans having equal length, is much unfavourable from the point of view of stability, since it gives rise to a *local minimum* of the instability thresholds. In the last part of the paper, we also briefly compare the energy thresholds of instability for a beam with one pier with the ones for a beam with two symmetric piers [4], concluding that two piers generally strengthen the structure, unless the ratio between the resulting spans is too small or too large (see the final part of Section 3).

Summing up, in the present work we prove some mathematical properties of the eigenvalue curves for a beam with an intermediate pier and we use the developed linear material to perform a stability analysis for a nonlinear model with a superquadratic (nonlocal) nonlinearity. In a similar way as for [4], this may be the starting point for the study of the stability of two-span suspension bridges. It is well understood that what generally occurs when such structures collapse (as for the Tacoma Narrows Bridge) is a sudden switch between two different oscillations, created by a significant transfer of energy from a longitudinal to a torsional mode. Here we are not concerned with torsional motions, yet the study of the stability of bi-modal longitudinal solutions may contribute to better understand why and how such energy exchanges take place. In principle, being more prone to longitudinal energy transfers may not necessarily represent a weakness in a real structure; however, the results in [4] seem to suggest that the stability portrait for two longitudinal modes of oscillation does not differ significantly from the one for a longitudinal versus a torsional oscillation (as in "degenerate plates"). Of course this point deserves further investigations.

Let us finally underline that, though the two-span configuration is more common for footbridges, it also occurs in real vehicular bridges: A few examples are the Second Kurushima bridge in Japan (according to [10]), with spans having a length of 1020m and 250m, the Xihoumen bridge in Zhejiang, China, with a main span of 1650m, and the North bridge in the Taizhou complex on the Yangtze river (China), with two equal spans having a length of 1080m each. Moreover, as the single-span configuration may be initially taken into consideration to model a three-span bridge with very short side spans, the two-span configuration could also be used in modeling long multi-span bridges with two main spans instead of a single one, like the Neuperlach footbridge in Munich (where the central spans are twice as long as the side ones). In this case one models the dynamics neglecting the lateral spans but focusing on the two central ones, separated by the internal pier.

2. One-pier hinged beams: Spectral theory

From now on, we consider a beam represented by an interval $I = [\alpha, \beta]$, where a third point $\sigma \in (\alpha, \beta)$ is fixed, determining the relative measure of the spans (see Figure 1).

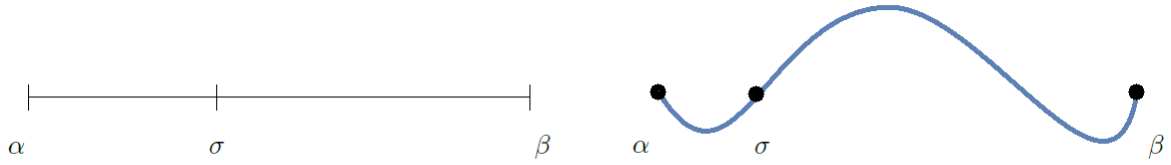

Figure 1. A beam with an intermediate pier.

In correspondence of the points α, σ, β, the displacement of the beam is set equal to zero. In this section, we determine the natural modes of vibration of such a structure under hinged boundary conditions (coming from the variational formulation below), namely with no bending at the endpoints, like in real suspension bridges.

The natural functional setting for Eq (1.1), taking into account the null-displacement conditions at α, σ, β, is here given by the space $V(I) = \{v \in H^2 \cap H_0^1(I) \mid v(\sigma) = 0\}$, where the constraint makes sense since $V(I) \subset C^0(\bar{I})$. Similarly as in [5, Theorems 1 and 2], the forced stationary problem $u'''' + \gamma u = g$ ($\gamma > 0$) enjoys well-posedness in $V(I)$ but the solutions are not C^4 due to the junction condition $u(\sigma) = 0$, which lowers the regularity to $C^2(\bar{I})$. For this reason, the weak formulation is here the only possible one. Accordingly, the eigenfunctions have to be searched by solving

$$\int_I e'' v'' = \mu \int_I ev, \qquad \text{for every } v \in V(I). \tag{2.1}$$

Through a regularity argument similar to the one in the proof of [5, Theorem 2], one can show that any eigenfunction belongs to $C^2(\bar{I})$ and is of class C^∞ on both spans $I_l = (\alpha, \sigma)$ and $I_r = (\sigma, \beta)$. Moreover, it necessarily satisfies the no-bending boundary conditions

$$e''(\alpha) = e''(\beta) = 0$$

at the endpoints of the beam. If $e \in V(I)$ is an eigenfunction, by taking $v = e$ in (2.1) one obtains that all the eigenvalues are strictly positive. Moreover, eigenfunctions corresponding to different eigenvalues are orthogonal in $L^2(I)$ and thus in $H^2(I)$. We thus set $\mu = \lambda^4$ and seek $e \in V(I)$ such that

$$\int_I e'' v'' = \lambda^4 \int_I ev, \qquad \text{for every } v \in V(I). \tag{2.2}$$

The following result holds.

Theorem 1. *The eigenvalues of* (2.1) *are simple; moreover, $\mu = \lambda^4$ is an eigenvalue if and only if $\lambda > 0$ satisfies the equality*

$$\sin[\lambda(\beta-\alpha)]\sinh[\lambda(\sigma-\alpha)]\sinh[\lambda(\beta-\sigma)] = \sinh[\lambda(\beta-\alpha)]\sin[\lambda(\sigma-\alpha)]\sin[\lambda(\beta-\sigma)]. \tag{2.3}$$

The corresponding eigenfunction e_λ has the following expression (up to the sign and to re-normalizations):

a) if $\lambda(\beta-\sigma)\in\mathbb{N}\pi$ (implying $\lambda(\beta-\alpha),\lambda(\sigma-\alpha)\in\mathbb{N}\pi$), then

$$e_\lambda(x)=\begin{cases}-\cos[\lambda(\beta-\sigma)]\sin[\lambda(x-\alpha)] & x\in I_l\\ \cos[\lambda(\sigma-\alpha)]\sin[\lambda(\beta-x)] & x\in I_r;\end{cases}$$

b) if $\lambda(\beta-\sigma)\notin\mathbb{N}\pi$ (implying $\lambda(\beta-\alpha),\lambda(\sigma-\alpha)\notin\mathbb{N}\pi$),

$$e_\lambda(x)=\begin{cases}\sinh[\lambda(\beta-\sigma)]\sin[\lambda(\beta-\sigma)]\{\sinh[\lambda(\sigma-\alpha)]\sin[\lambda(x-\alpha)]-\sin[\lambda(\sigma-\alpha)]\sinh[\lambda(x-\alpha)]\} & x\in I_l\\ \sinh[\lambda(\sigma-\alpha)]\sin[\lambda(\sigma-\alpha)]\{\sinh[\lambda(\beta-\sigma)]\sin[\lambda(\beta-x)]-\sin[\lambda(\beta-\sigma)]\sinh[\lambda(\beta-x)]\} & x\in I_r.\end{cases}$$

Proof. Similarly as in [5], we have that any eigenfunction solves the linear equation $e''''=\lambda^4 e$ on each span, hence we seek the eigenfunctions as linear combinations of trigonometric and hyperbolic functions on the two intervals I_l and I_r:

$$e_\lambda(x)=\begin{cases}a\cos\lambda x+b\sin\lambda x+c\cosh\lambda x+d\sinh\lambda x & x\in I_l\\ A\cos\lambda x+B\sin\lambda x+C\cosh\lambda x+D\sinh\lambda x & x\in I_r.\end{cases}$$

Imposing the vanishing and the no-bending conditions in α,β and imposing the vanishing and the C^2-junction conditions in σ results into the following system of eight equations:

$$\begin{cases}a\cos\lambda\alpha+b\sin\lambda\alpha=0\\ c\cosh\lambda\alpha+d\sinh\lambda\alpha=0\\ A\cos\lambda\beta+B\sin\lambda\beta=0\\ C\cosh\lambda\beta+D\sinh\lambda\beta=0\\ a\cos\lambda\sigma+b\sin\lambda\sigma+c\cosh\lambda\sigma+d\sinh\lambda\sigma=0\\ A\cos\lambda\sigma+B\sin\lambda\sigma+C\cosh\lambda\sigma+D\sinh\lambda\sigma=0\\ -a\sin\lambda\sigma+b\cos\lambda\sigma+c\sinh\lambda\sigma+d\cosh\lambda\sigma=-A\sin\lambda\sigma+B\cos\lambda\sigma+C\sinh\lambda\sigma+D\cosh\lambda\sigma\\ -a\cos\lambda\sigma-b\sin\lambda\sigma+c\cosh\lambda\sigma+d\sinh\lambda\sigma=-A\cos\lambda\sigma-B\sin\lambda\sigma+C\cosh\lambda\sigma+D\sinh\lambda\sigma,\end{cases}$$

the resolution of which leads to the conclusion. □

In the previous statement, a) corresponds to the case when the equality (2.3) is fulfilled with both sides equal to 0. This is the only case in which $e_\lambda\in C^\infty(I)$; in particular, if $\lambda\alpha,\lambda\beta,\lambda\sigma\in\mathbb{N}\pi$, one simply has (up to multiplicative constants) $e_\lambda(x)=\sin(\lambda x)$. In the case $\sigma=(\alpha+\beta)/2$, Theorem 1 reads as follows.

Corollary 2. *Let $\sigma=(\alpha+\beta)/2$. The eigenvalues $\mu=\lambda^4$ of* (2.1) *are completely determined by the numbers $\lambda>0$ satisfying*

$$\cos\left[\lambda\left(\frac{\beta-\alpha}{2}\right)\right]\sinh\left[\lambda\left(\frac{\beta-\alpha}{2}\right)\right]=\sin\left[\lambda\left(\frac{\beta-\alpha}{2}\right)\right]\cosh\left[\lambda\left(\frac{\beta-\alpha}{2}\right)\right].$$

In particular, if $\alpha=-\pi$, $\beta=\pi$, such an equality reads as

$$\cos\lambda\pi\sinh\lambda\pi=\sin\lambda\pi\cosh\lambda\pi.$$

Condition (2.3) thus characterizes the couples (σ, λ) for which λ^4 is an eigenvalue of (2.2). Of course, such a condition is "symmetric with respect to $(\alpha+\beta)/2$", so that the eigenvalues associated with a fixed $\sigma \in (\alpha, (\alpha+\beta)/2)$ are the same as the ones associated with $\alpha+\beta-\sigma$. Furthermore, the eigenvalues of (2.1) can be immediately related with the (odd) eigenvalues of a beam with two symmetric internal piers, as the one studied in [5], where it was assumed that $\alpha = -\pi$, $\beta = \pi$ to simplify the computations. By setting

$$\Lambda = \frac{\lambda(\beta-\alpha)}{\pi}, \qquad a = \frac{\sigma-\alpha}{\beta-\alpha} \in (0,1), \tag{2.4}$$

(2.3) reads indeed as

$$\sin(\Lambda\pi)\sinh(\Lambda a\pi)\sinh[\Lambda(1-a)\pi] = \sinh(\Lambda\pi)\sin(\Lambda a\pi)\sin[\Lambda(1-a)\pi],$$

which coincides with formula (3.3) in [5]. This means that the eigenvalues of (2.2) are exactly the eigenvalues of the beam with two symmetric piers at the points $\pm(\sigma+\pi)/2\pi$, *divided by* 2. We also notice that through the change of variables (2.4), together with the rescaling

$$X = \frac{\pi(x-\alpha)}{\beta-\alpha}, \tag{2.5}$$

the eigenfunction $e_\lambda(x)$ takes the form of $\mathscr{O}_\Lambda(X)$ defined in [5, Theorem 6]. Namely, up to rescaling (and to a multiplicative factor), the eigenfunctions of the problem with one pier are exactly the *odd eigenfunctions* of the problem with two symmetric piers, considered only *on a half-interval*; indeed, it is crucial that the odd function $\mathscr{O}_\Lambda$ vanishes at 0 (with null second derivative), so that we can determine a bijection between the smaller beam $[0,\pi]$ considered in [5] – which encloses exactly one pier – and $[\alpha,\beta]$, preserving the conditions at the endpoints and at the pier. From [5] we can thus draw several properties of the eigenvalue curves and of the eigenfunctions; in order to state them, it is convenient to denote by Λ_n^c the eigenvalues of the problem

$$u'''' = \lambda^4 u,\ u(\alpha) = u'(\alpha) = 0,\ u(\beta) = u''(\beta) = 0,$$

namely the eigenvalues for a single beam (with *no piers*) which is clamped on the left and hinged on the right (compare with Section 3 below). Such numbers are given by the λ's solving

$$\sin[\lambda(\beta-\alpha)]\cosh[\lambda(\beta-\alpha)] = \cos[\lambda(\beta-\alpha)]\sinh[\lambda(\beta-\alpha)],$$

with corresponding eigenfunction given, on the interval $[\alpha,\beta]$, by

$$e_{\Lambda_n^c}(x) = \sinh[\Lambda_n^c(\beta-\alpha)]\sin[\Lambda_n^c(\beta-x)] - \sin[\Lambda_n^c(\beta-\alpha)]\sinh[\Lambda_n^c(\beta-x)].$$

These eigenvalues coincide with the ones for the (clamped on the right and hinged on the left) problem

$$u'''' = \lambda^4 u,\ u(\alpha) = u''(\alpha) = 0,\ u(\beta) = u'(\beta) = 0,$$

with corresponding eigenfunction which may be easily obtained from the previous one by symmetry.

Proposition 3. *The equality* (2.3) *implicitly defines a countable set of regular curves $\lambda = \lambda(\sigma)$; for each of such curves, there exists n so that $\lambda(\sigma) \to \Lambda_n^c$ for $\sigma \to \alpha$ (and, by symmetry, also for $\sigma \to \beta$); this correspondence is* 1*-to-*1.

Proof. In view of the previous comments, the proof can be desumed from [5, Lemmas 15 and 16]. □

We can thus arrange the eigenvalue curves into a sequence $\lambda = \lambda_n(\sigma)$, labeling the corresponding eigenfunctions by $e_n(\sigma)$. We can also give a complete characterization of the nodal properties of the eigenfunctions, similarly as in [5, Section 3.2]; defining the index of an eigenfunction e_λ as

$$i(e_\lambda) = \begin{cases} \#\{x \in I_l \cup I_r \mid e_\lambda(x) = 0\} & \text{if } e'_\lambda(\sigma) \neq 0 \\ \#\{x \in I_l \cup I_r \mid e_\lambda(x) = 0\} + 1 & \text{if } e'_\lambda(\sigma) = 0, \end{cases}$$

we have the following counterpart of [5, Theorem 10].

Proposition 4. *For every n, it holds that* $i(e_n) = n$.

Denoting by E_n, $n = 0, 1, \ldots$, all the eigenfunctions (even and odd) introduced in [5], the statement is obtained by recalling (2.4) and (2.5), so that

$$E_{2n+1}(x) = e_n\left(\alpha + \frac{\beta - \alpha}{\pi} x\right), \quad x \in [0, \pi];$$

hence, since [5, Theorem 10] ensures that E_{2n+1} has n internal zeros in $[0, \pi]$, the same is for e_n on $[\alpha, \beta]$. In Figure 2, we depict some of the eigenvalue curves for the choices $\alpha = 0, \beta = 4$ (left) and $\alpha = -\pi, \beta = \pi$ (right). In Figures 3 and 4 we instead depict the first twelve eigenfunctions of problem (2.2) for the choices $\alpha = 0, \beta = 4, \sigma = 3$ and $\alpha = -\pi, \beta = \pi, \sigma = 0$.

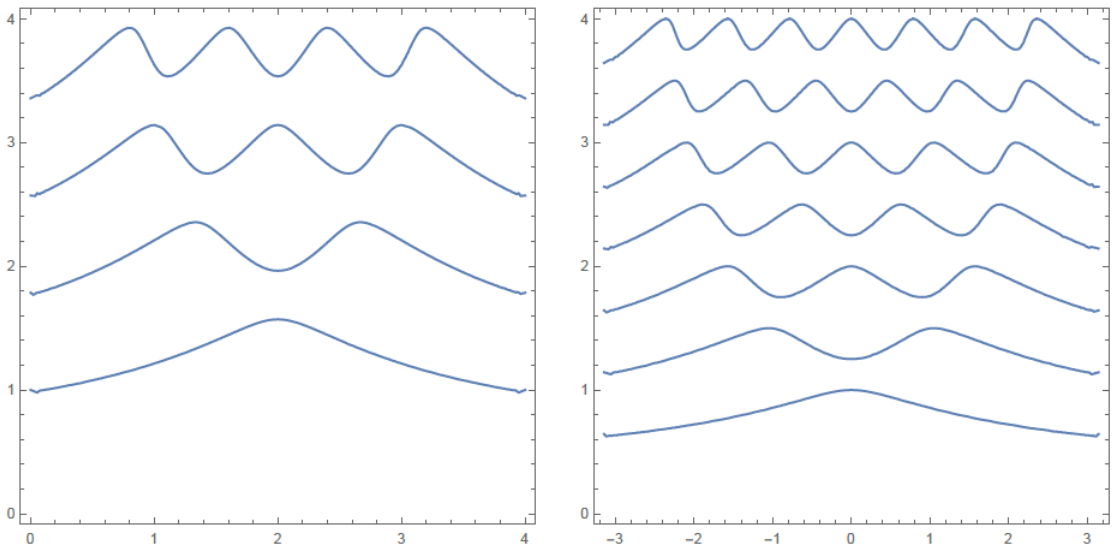

Figure 2. The curves implicitly defined by (2.3) in the regions $(\sigma, \lambda) \in (0, 4) \times (0, 4)$ (left, for $\alpha = 0$ and $\beta = 4$) and $(\sigma, \lambda) \in (-\pi, \pi) \times (0, 4)$ (right, for $\alpha = -\pi, \beta = \pi$).

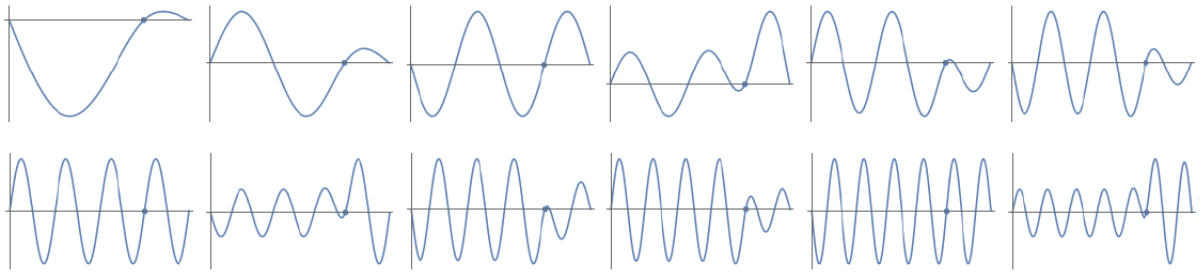

Figure 3. The shape of the first twelve eigenfunctions for $\alpha = 0, \beta = 4, \sigma = 3$.

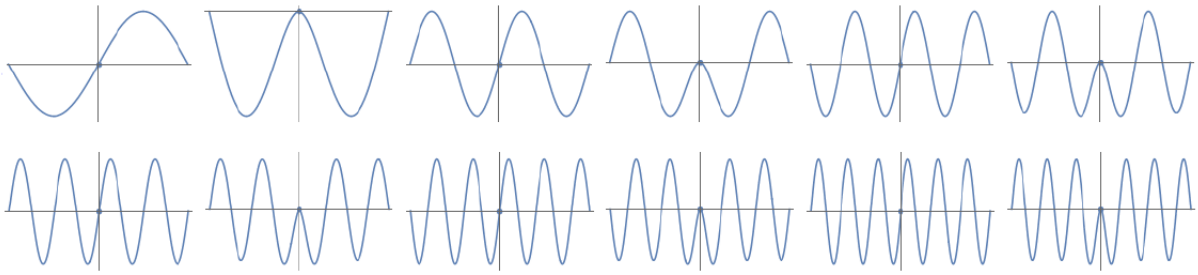

Figure 4. The shape of the first twelve eigenfunctions for $\alpha = -\pi, \beta = \pi, \sigma = 0$.

In Figure 4, we recognize the fourth eigenfunction as the eigenfunction of the problem hinged at the endpoints and clamped in 0, already mentioned in [5]; this is an example of eigenfunction with a double zero in the pier. In order for an eigenfunction to have a double zero in the pier, at the same time it has to be

$$\sinh[\lambda(\sigma-\alpha)]\cos[\lambda(\sigma-\alpha)] = \sin[\lambda(\sigma-\alpha)]\cosh[\lambda(\sigma-\alpha)] \tag{2.6}$$

and

$$\sinh[\lambda(\beta-\sigma)]\cos[\lambda(\beta-\sigma)] = \sin[\lambda(\beta-\sigma)]\cosh[\lambda(\beta-\sigma)], \tag{2.7}$$

namely

$$\tan[\lambda(\sigma-\alpha)] = \tanh[\lambda(\sigma-\alpha)], \qquad \tan[\lambda(\beta-\sigma)] = \tanh[\lambda(\beta-\sigma)].$$

We now show that such a case, together with the one of C^∞-eigenfunctions, corresponds to a critical point on the eigenvalue curves.

Theorem 5. *Let $\lambda = \lambda(\sigma)$ be the eigenvalue curves implicitly defined by* (2.3)*, see Proposition 3. Then, $\lambda'(\sigma) = 0$ if and only if*

- *either $\lambda(\beta-\alpha), \lambda(\beta-\sigma), \lambda(\sigma-\alpha) \in \mathbb{N}\pi$, corresponding to case a) in the statement of Theorem 1 (and hence the associated eigenfunction belongs to $C^4(I)$);*

- *or* (2.6) *and* (2.7) *are fulfilled at the same time (and hence the corresponding eigenfunction has a double zero in* σ*).*

The former case occurs if and only if σ *is a maximum point for* $\lambda(\cdot)$*, while the latter takes place if and only if* σ *is a minimum point for* $\lambda(\cdot)$*.*

Proof. By the Implicit Function Theorem, setting

$$F(\lambda,\sigma)=\sin[\lambda(\beta-\alpha)]\sinh[\lambda(\sigma-\alpha)]\sinh[\lambda(\beta-\sigma)]-\sinh[\lambda(\beta-\alpha)]\sin[\lambda(\sigma-\alpha)]\sin[\lambda(\beta-\sigma)],$$

on the eigenvalue curves one has that

$$\lambda'(\sigma)=-\frac{F_\sigma(\lambda(\sigma),\sigma)}{F_\lambda(\lambda(\sigma),\sigma)}\quad\Rightarrow\quad\lambda'(\sigma)=0\quad\Longleftrightarrow\quad F_\sigma(\lambda(\sigma),\sigma)=0.$$

Since

$$F_\sigma(\lambda,\sigma)=\lambda\{\sin[\lambda(\beta-\alpha)]\sinh[\lambda(\beta+\alpha-2\sigma)]-\sinh[\lambda(\beta-\alpha)]\sin[\lambda(\beta+\alpha-2\sigma)]\},$$

if $F_\sigma(\lambda,\sigma)=0$ then it has to be

$$\sin[\lambda(\beta-\alpha)]\sinh[\lambda(\beta+\alpha-2\sigma)]=\sinh[\lambda(\beta-\alpha)]\sin[\lambda(\beta+\alpha-2\sigma)].$$

If such an equality is fulfilled with both sides equal to 0, we have $\lambda(\beta-\alpha)\in\mathbb{N}\pi$, automatically implying that $\lambda(\beta-\sigma)$, $\lambda(\sigma-\alpha)\in\mathbb{N}\pi$ in view of (2.3). Referring to the statement of Theorem 1, this means that we are in case a). Otherwise, we write

$$\beta-\alpha=(\beta-\sigma)+(\sigma-\alpha),\qquad\beta+\alpha-2\sigma=(\beta-\sigma)-(\sigma-\alpha),\tag{2.8}$$

so that

$$\sin[\lambda(\sigma-\alpha)]\cos[\lambda(\beta-\sigma)]\sinh[\lambda(\beta-\sigma)]\cosh[\lambda(\sigma-\alpha)]=\sin[\lambda(\beta-\sigma)]\cos[\lambda(\sigma-\alpha)]\sinh[\lambda(\sigma-\alpha)]\cosh[\lambda(\beta-\sigma)],\tag{2.9}$$

while (2.3) ensures that

$$\begin{aligned}&\sin[\lambda(\sigma-\alpha)]\sinh[\lambda(\sigma-\alpha)]\Big\{\cos[\lambda(\beta-\sigma)]\sinh[\lambda(\beta-\sigma)]-\sin[\lambda(\beta-\sigma)]\cosh[\lambda(\beta-\sigma)]\Big\}\\&=\sin[\lambda(\beta-\sigma)]\sinh[\lambda(\beta-\sigma)]\Big\{\sin[\lambda(\sigma-\alpha)]\cosh[\lambda(\sigma-\alpha)]-\cos[\lambda(\sigma-\alpha)]\sinh[\lambda(\sigma-\alpha)]\Big\}.\end{aligned}\tag{2.10}$$

By making $\sinh[\lambda(\sigma-\alpha)]\cosh[\lambda(\beta-\sigma)]$ and $\sin[\lambda(\beta-\sigma)]\cos[\lambda(\sigma-\alpha)]$ explicit from (2.9) and inserting into (2.10), we find the relation

$$\frac{\sinh[\lambda(\beta-\sigma)]}{\cosh[\lambda(\beta-\sigma)]}-\frac{\sin[\lambda(\sigma-\alpha)]}{\cos[\lambda(\sigma-\alpha)]}=\frac{\sin[\lambda(\beta-\sigma)]}{\cos[\lambda(\beta-\sigma)]}-\frac{\sinh[\lambda(\sigma-\alpha)]}{\cosh[\lambda(\sigma-\alpha)]},$$

which together with (2.9) provides (excluding the impossible case $\tanh[\lambda(\sigma-\alpha)]=-\tanh[\lambda(\beta-\sigma)]$)

$$\tan[\lambda(\sigma-\alpha)]=\tanh[\lambda(\sigma-\alpha)],\quad\tan[\lambda(\beta-\sigma)]=\tanh[\lambda(\beta-\sigma)],\tag{2.11}$$

concluding the first part of the statement.

Let us now characterize the nature of the critical points. First, since

$$F_{\sigma\sigma}(\lambda,\sigma) = 2\lambda^2(\cos[\lambda(\beta+\alpha-2\sigma)]\sinh[\lambda(\beta-\alpha)] - \sin[\lambda(\beta-\alpha)]\cosh[\lambda(\beta+\alpha-2\sigma)])$$

and

$$\begin{aligned} F_\lambda(\lambda,\sigma) = {} & (\beta+\alpha-2\sigma)\Big(\sin[\lambda(\beta-\alpha)]\cosh[\lambda(\beta-\sigma)]\sinh[\lambda(\sigma-\alpha)] - \sinh[\lambda(\beta-\alpha)]\cos[\lambda(\beta-\sigma)]\sin[\lambda(\sigma-\alpha)]\Big) \\ & +(\beta-\alpha)\Big(\cos[\lambda(\beta-\alpha)]\sinh[\lambda(\sigma-\alpha)]\sinh[\lambda(\beta-\sigma)] - \cosh[\lambda(\beta-\alpha)]\sin[\lambda(\sigma-\alpha)]\sin[\lambda(\beta-\sigma)]\Big), \end{aligned}$$

if $\lambda(\beta-\alpha)$, $\lambda(\beta-\sigma)$, $\lambda(\sigma-\alpha) \in \mathbb{N}\pi$ then one finds that

$$F_{\sigma\sigma}(\lambda,\sigma) = 2\lambda^2 \sinh[\lambda(\beta-\alpha)]\cos[\lambda(\sigma-\alpha)]\cos[\lambda(\beta-\sigma)]$$

and

$$F_\lambda(\lambda,\sigma) = (\beta-\alpha)\cos[\lambda(\beta-\alpha)]\sinh[\lambda(\sigma-\alpha)]\sinh[\lambda(\beta-\sigma)],$$

so that

$$\lambda''(\sigma) = -\frac{F_{\sigma\sigma}(\lambda(\sigma),\sigma)}{F_\lambda(\lambda(\sigma),\sigma)} < 0,$$

taking into account that in this case $\cos[\lambda(\beta-\sigma)]\cos[\lambda(\sigma-\alpha)] = \cos[\lambda(\beta-\alpha)]$. It follows that C^4-eigenfunctions correspond to *maxima* on the eigenvalue curves. On the other hand, multiplying side by side the two equalities in (2.11) and inserting into (2.3) we obtain

$$\sin[\lambda(\beta-\alpha)]\cosh[\lambda(\sigma-\alpha)]\cosh[\lambda(\beta-\sigma)] = \sinh[\lambda(\beta-\alpha)]\cos[\lambda(\sigma-\alpha)]\cos[\lambda(\beta-\sigma)]; \quad (2.12)$$

expanding the expression of $F_{\sigma\sigma}$ and replacing (2.12) therein we find that $F_{\sigma\sigma}$ has the same sign as $\sin[\lambda(\beta-\alpha)]$. Using again (2.8) and (2.11) - this last one in order to replace $\sin[\lambda(\sigma-\alpha)]\cosh[\lambda(\sigma-\alpha)]$ by $\sinh[\lambda(\sigma-\alpha)]\cos[\lambda(\sigma-\alpha)]$ and $\sin[\lambda(\beta-\sigma)]\cosh[\lambda(\beta-\sigma)]$ by $\sinh[\lambda(\beta-\sigma)]\cos[\lambda(\beta-\sigma)]$ - one finds that

$$F_\lambda(\lambda,\sigma) = -2(\beta-\alpha)\sin[\lambda(\sigma-\alpha)]\sin[\lambda(\beta-\sigma)]\sinh[\lambda(\sigma-\alpha)]\sinh[\lambda(\beta-\sigma)],$$

which in view of (2.3) has opposite sign with respect to $\sin[\lambda(\beta-\alpha)]$. Hence, $\lambda''(\sigma) > 0$ and σ is a minimum point for $\lambda(\cdot)$, as desired. □

Theorem 5 also allows to determine whether an eigenfunction can be sign-definite (out of the pier). To this end, notice that in this case the eigenfunction has to display a unique double zero in correspondence of the pier; hence, the corresponding couples $(\sigma,\lambda(\sigma))$ have to lie on the eigenvalue curve $\lambda = \lambda_1(\sigma)$ (the second one), thanks to Proposition 4, and will be found in correspondence of the minima therein. We thus have the following.

Corollary 6. *For the choice $\sigma = \sigma_m := \frac{\alpha+\beta}{2}$, $e_1(\sigma)$ is sign-definite out of the pier; this is the only possibility for an eigenfunction of* (2.2) *to be sign-definite.*

Proof. As for the first part of the proof, on the one hand we observe that σ_m is always a critical point for $\sigma \mapsto \lambda(\sigma)$, since the eigenvalue curves are regular and symmetric with respect to σ_m; on the other hand, σ_m cannot be a maximum on the second eigenvalue curve, since the nodal condition $i(e_1) = 1$ has to hold and no trigonometric function has double zeros. Thus, e_1 is sign-definite out of the pier for

$\sigma = \sigma_m$. To show that there cannot be other minima on the second eigenvalue curve, recalling case a) in the statement of Theorem 1, Proposition 3 and Proposition 4 we note explicitly that the maximum value of λ on the 0-th eigenvalue curve is given by $\lambda(\sigma_m) = 2\pi/(\beta - \alpha)$, while the maximum on the subsequent curve is given by $\lambda = 3\pi/(\beta - \alpha) =: \lambda_{\max}$, for $\sigma = (2\alpha + \beta)/3$ or $\sigma = (2\beta + \alpha)/3$. If there were minima σ other than σ_m on the curve $\lambda = \lambda_1(\sigma)$, then it would be

$$\tan[\lambda(\beta - \sigma)] = \tanh[\lambda(\beta - \sigma)], \qquad \tan[\lambda(\sigma - \alpha)] = \tanh[\lambda(\sigma - \alpha)].$$

Assuming $\sigma > (\beta+\alpha)/2$ without loss of generality, then it should be $\lambda(\beta-\sigma) = S_i$, $\lambda(\sigma-\alpha) = S_j > S_i$, where S_i and S_j are two zeros of the function $x \mapsto \tan(x)-\tanh(x)$. This would give $\lambda = (S_i+S_j)/(\beta-\alpha)$ and the least value of this sum is approximately $10.99/(\beta - \alpha) > 3\pi/(\beta - \alpha) = \lambda_{\max}$, which is a contradiction. □

The procedure used to prove Corollary 6 can be refined in order to count the number of critical points on each eigenvalue curve; recalling (2.4), it is here more convenient to work with $\alpha = -\pi, \beta = \pi$ and write $\sigma = s\pi$, $s \in [0, 1)$, reasoning on the half-interval $(-\pi, 0]$ by symmetry. In this case, since $\beta - \alpha = 2\pi$, in view of case a) of Theorem 1 the maximum values on the eigenvalue curves are equal to

$$\lambda_{k,\max} = \frac{k+2}{2}, \quad k = 0, 1, \dots \tag{2.13}$$

and $\lambda(1 + s), \lambda(1 - s) \in \mathbb{N}$, so that for each maximum value as in (2.13) it has to be $(k+2)(1 \pm s)/2 \in \mathbb{N}$. Therefore, $(k + 2)s$ has to be an integer and have the same parity as k; hence, the possible choices of σ yielding $\lambda(\sigma) = \lambda_{k,\max}$ are given by $\sigma = s\pi$ with

$$s = \frac{\ell}{k+2}, \quad \text{for every } \ell \in \mathbb{N},\ \ell < k + 2 \text{ such that } \ell \bmod 2 = k \bmod 2. \tag{2.14}$$

There are $[(k + 1)/2]$ of such choices of $\sigma > 0$ (where $[\cdot]$ denotes the integer part); $\sigma = 0$ has to be included if and only if k is even. Hence, fixed k there are $2[(k + 1)/2] + (k + 1) \bmod 2 = k + 1$ different maximum points on the eigenvalue curves; in correspondence of such points, $\sigma \mapsto \lambda(\sigma)$ takes the value $\lambda_{k,\max}$. For $\lambda = \lambda_{k,\max}$, the explicit expression of the associated C^4-eigenfunction e_λ (which is a trigonometric function, recall Theorem 1) shows that $i(e_\lambda) = k$, so that they all have to lie on the same curve, the one which approaches Λ_k^c for $\sigma \to \pm\pi$. Hence, on the k-th curve there are exactly $k + 1$ local maxima. Since between two local maxima there has to be a minimum, on the k-th curve there have to be at least k minima; to show that they are exactly k, we first observe that the couple (σ, λ) will correspond to a local minimum if and only if, at the same time,

$$\lambda(1 - s)\pi = S_i, \quad \lambda(1 + s)\pi = S_j, \quad (S_i \le S_j),$$

for suitable integers $i \le j$. We recall that $\{S_i\}_i$ denotes the sequence of zeros of the function $x \mapsto \tan(x) - \tanh(x)$. This yields

$$\lambda = \frac{S_i + S_j}{2\pi}, \quad \sigma = \frac{(S_j - S_i)\pi}{S_i + S_j}$$

and the minima below $\lambda_{k,\max}$ (in the region $\sigma \ge 0$) correspond to all the couples (i, j) for which

$$\frac{S_i + S_j}{2\pi} \le \frac{k+2}{2}.$$

We now use the approximation

$$S_i \approx 2\pi\left(\frac{i+1}{2}+\frac{1}{8}\right), \quad i=0,1,2,\ldots, \tag{2.15}$$

which works up to an error of at most $4\cdot 10^{-4}$ ($\tanh(s)$ rapidly converges to 1 and is increasing, so it is sufficient to control the error on S_0). Hence,

$$\lambda \approx \frac{i+j}{2}+\frac{5}{4}, \quad i=0,1,\ldots, \quad j=0,1,\ldots, \quad i\le j$$

and the minima below $\lambda_{k,\max}$ are then obtained for the couples of integers (i,j), with $0\le i\le j$, such that

$$\frac{i+j}{2}+\frac{5}{4}\le\frac{k+2}{2} \qquad \Rightarrow i+j+\frac{1}{2}<k \Rightarrow i+j<k. \tag{2.16}$$

This actually makes the approximation (2.15) legitimate, since $(S_i+S_j)/2\pi$ cannot differ from $(i+j)/2+5/4$ more than $2\cdot 10^{-4}$, so the inequality in (2.16) would hold all the same for S_i, S_j (in place of their approximations). As can be proved by induction, the number of couples (i,j) fulfilling (2.16) is given by

$$n_+(k)=\begin{cases}\left[\frac{k}{2}\right]\left(k-\left[\frac{k}{2}\right]+1\right)=\frac{k}{2}\left(\frac{k}{2}+1\right) & \text{if } k \text{ is even,}\\ \left(k-\left[\frac{k}{2}\right]\right)\left(\left[\frac{k}{2}\right]+1\right)=\left(\frac{k+1}{2}\right)^2 & \text{if } k \text{ is odd.}\end{cases}$$

In particular, $n_+(0)=0$ and $n_+(1)=1$, as we have already seen in the proof of Corollary 6; more in general, the number of minimum points which lie on the curve $\lambda=\lambda_k(\sigma)$ in the region $\sigma\ge 0$ is given by

$$n_+(k)-n_+(k-1)=\left[\frac{k+1}{2}\right],$$

corresponding to the couples of integers (i,j) for which $i+j=k-1$. Recalling that $\sigma=0$ is always a critical point and corresponds to a minimum only for k odd in view of (2.14), the number of minimum points $n_{\min}(k)$ lying on the curve $\lambda=\lambda_k(\sigma)$ is thus given by

$$n_{\min}(k)=2\left[\frac{k+1}{2}\right]-k \bmod 2 = k.$$

Finally, we can now infer that the local minima on the k-th eigenvalue curve are found at the level

$$\lambda\approx\frac{k-1}{2}+\frac{5}{4}=\frac{k}{2}+\frac{3}{4}>\Lambda_k^c\approx\frac{k+1}{2}+\frac{1}{8}=\frac{k}{2}+\frac{5}{8}.$$

Summing up, since the rescaling (2.4) does not modify the number and the nature of the critical points, we have proved the following.

Theorem 7. *On the eigenvalue curve $\lambda=\lambda_k(\sigma)$, $k=0,1,...$, there are k local minima and $k+1$ local maxima. Moreover, the following estimate holds for every choice of σ:*

$$\left(\frac{k}{2}+\frac{5}{8}\right)\approx\Lambda_k^c\le\lambda_k(\sigma)\le\frac{k}{2}+1.$$

This says that the width of the spectral gaps is here bounded from below by some explicit positive constant, contrary to what occurs for a beam with two symmetric piers, for which different modes can have similar frequencies. Of course, as for the case of a beam with two symmetric piers, one has that $\lim_{k\to+\infty} \frac{\lambda_{k+1}(\sigma)}{\lambda_k(\sigma)} = 1$.

We close the section by observing that if $I = [-\pi, \pi]$ represents a beam with two internal piers at $\pm a\pi$, $a \in (0, 1)$ (as in [5]), one could use a similar procedure as the one performed before to infer that on the eigenvalue curve $\lambda = \lambda_k(a)$ there are exactly $[k/2]$ minima and $[(k + 2)/2]$ maxima. Similarly as in Theorem 5, one can prove the previous correspondence between critical points on the eigenvalue curves and peculiar properties of the corresponding eigenfunctions (C^4/having double zeros in the piers). This relationship could probably be framed into some optimal partition scheme and hold for a general problem with multi-point conditions, as suggested by the considerations in the next section about the clamped problem, as well. This point deserves further investigation.

3. A superquadratic displacement problem: Stability and optimal geometry of the structure

From now on, for simplicity of computation we assume that $\alpha = -\pi$, $\beta = \pi$, so that $I = [-\pi, \pi]$. In this section, we are interested in the evolution equation

$$u_{tt} + u_{xxxx} + \|u\|_{L^2}^2 u = 0, \tag{3.1}$$

for $x \in I$ and $t > 0$. Eq (3.1) can be obtained by imposing the preservation of the energy

$$\mathcal{E}(u) = \frac{1}{2}\left(\int_I u_t^2 + \int_I u_{xx}^2\right) + \frac{1}{4}\left(\int_I u^2\right)^2,$$

where the first and the second term correspond to the kinetic and to the bending energy of the beam, while the last summand is a nonlinear term describing a stiffened beam where the displacement behaves superquadratically and nonlocally (see for instance [2]). This means that the restoring force is distributed along the whole length of the beam and any displacement of the beam from its equilibrium position increases the resistance to further displacement in all the other points. In front of such an expression, one could introduce a positive coefficient γ, representing - in a suspension bridge perspective - the tension of the cables at rest; however, the rescaling $v = \sqrt{\gamma}u$ allows us to set $\gamma = 1$ without loss of generality.

Definition 8. *We say that $u \in C^0(\mathbb{R}_+; V(I)) \cap C^1(\mathbb{R}_+; L^2(I)) \cap C^2(\mathbb{R}_+; V'(I))$ is a (weak) solution of* (3.1) *if $u(\cdot, 0) \in V(I)$, $u_t(\cdot, 0) \in L^2(I)$ and*

$$\langle u_{tt}, v\rangle + \int_I u_{xx} v'' + \|u\|_{L^2}^2 \int_I uv = 0,$$

for every $v \in V(I)$ and every $t > 0$.

Here $V(I)$ denotes the functional space introduced in the previous section, and $\langle\cdot,\cdot\rangle$ denotes the duality between $V'(I)$ and $V(I)$. The functional setting takes into account the boundary/internal conditions which we will associate with (3.1):

$$u(-\pi, t) = u(\pi, t) = u(\sigma, t) = 0, \qquad t \geq 0.$$

The well-posedness of the problem in the space $V(I)$ can be proved similarly as in [4]. We are interested in analyzing the energy thresholds of instability for bi-modal solutions of (3.1), namely solutions having the form

$$u(x,t) = w(t)e_\lambda(x) + z(t)e_\rho(x), \tag{3.2}$$

where e_λ and e_ρ are two different eigenfunctions, in dependence on the position of the internal pier and on the considered boundary conditions at the endpoints (so that the eigenvalues λ, ρ and the associated eigenfunctions may correspond to different boundary value problems). Besides the hinged boundary conditions, discussed in the previous section, we will also consider clamped boundary conditions

$$u(-\pi,t) = u'(-\pi,t) = u(\pi,t) = u'(\pi,t) \equiv 0$$

and left-clamped and right-hinged (or vice versa, by symmetry) boundary conditions

$$u(-\pi,t) = u'(-\pi,t) = u(\pi,t) = u''(\pi,t) \equiv 0.$$

In the first case, the space in which framing the problem variationally is given by

$$V_0(I) = \{u \in H_0^2(I) \mid u(\sigma) = 0\},$$

while in the second one it is

$$V_*(I) = \{u \in H^2 \cap H_0^1(I) \mid u'(-\pi) = 0, u(\sigma) = 0\}.$$

The right-hinged boundary condition in the second case derives from the variational formulation of the problem. The well-posedness of (3.1) in the spaces V_0 and V_*, with the corresponding boundary conditions, can be proved similarly as in [4] as well, once a suitable basis of eigenfunctions for the corresponding linear stationary problem is provided. However, in all of these cases one has that the eigenfunctions of the linear stationary problem belong to $C^2(\bar{I}) \cap C^4(\overline{I_l}) \cap C^4(\overline{I_r})$ (using for instance [11]), and hence it is possible to seek them as in the proof of Theorem 1. According to this scheme, the following theorems then hold.

Theorem 9. *The eigenvalues of the clamped problem*

$$\int_I u''v'' = \mu \int_I uv, \quad \text{for every } v \in V_0(I) \tag{3.3}$$

are simple; moreover, $\mu = \lambda^4$ is an eigenvalue if and only if $\lambda > 0$ satisfies the equality

$$2(\sinh[\lambda(\pi-\sigma)]\cos[\lambda(\pi-\sigma)] + \sinh[\lambda(\pi+\sigma)]\cos[\lambda(\pi+\sigma)] - \sin[\lambda(\pi-\sigma)]\cosh[\lambda(\pi-\sigma)] - \sin[\lambda(\pi+\sigma)]\cosh[\lambda(\pi+\sigma)])$$

$$= \sinh(2\lambda\pi)(\cos 2\lambda\sigma + \cos 2\lambda\pi) - \sin(2\lambda\pi)(\cosh 2\lambda\sigma + \cosh 2\lambda\pi).$$

We omit writing the form of the corresponding eigenfunctions, which is quite involved; we only give an overview of their shape by depicting the first twelve of them for the choice $\sigma = \pi/10$ (Figure 5).

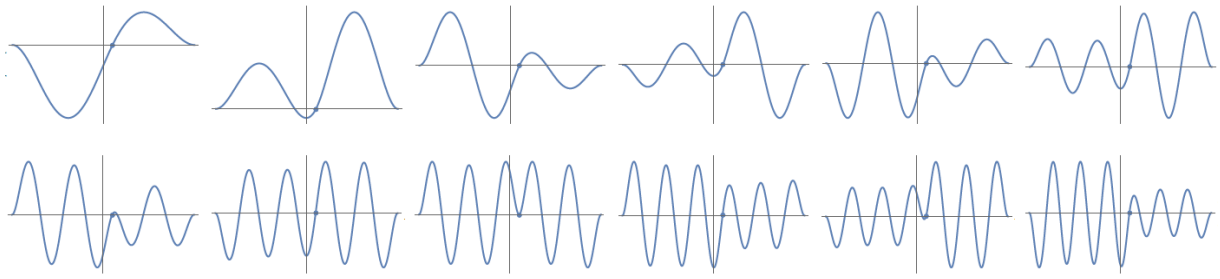

Figure 5. The shape of the first twelve eigenfunctions of the clamped problem (3.3) with $\sigma = \pi/10$.

We observe that if λ^4 is an eigenvalue of the clamped problem, the corresponding eigenfunction e_λ is of class C^4 if and only if

$$\tan(\lambda\pi) = \tanh(\lambda\pi) \quad \text{or} \quad \tan(\lambda\pi) = -\tanh(\lambda\pi) \tag{3.4}$$

and has, respectively, the expression

$$e_\lambda(x) = \sinh(\lambda\pi)\sin(\lambda x) - \sin(\lambda\pi)\sinh(\lambda x) \quad \text{or} \quad e_\lambda(x) = \sinh(\lambda\pi)\cos(\lambda x) + \sin(\lambda\pi)\cosh(\lambda x).$$

On the other hand, by direct computation (see the proof of Theorem 1) it may be seen that e_λ has a double zero at σ if and only if

$$\cos[\lambda(\pi+\sigma)]\cosh[\lambda(\pi+\sigma)] = 1. \tag{3.5}$$

Again, it may be seen that (3.4) and (3.5) occur exactly in correspondence, respectively, of maximum and minimum points on the eigenvalue curves. We do not give a proof similar to the one of Theorem 5, but we show a numerical evidence (Figure 6, left picture) in the (σ, λ)-plane, where the blue lines are the eigenvalue curves, the green lines are the curves implicitly defined by (3.4) and the orange lines are the curves implicitly defined by (3.5).

Theorem 10. *The eigenvalues of the left-clamped and right-hinged problem*

$$\int_I u''v'' = \mu \int_I uv, \quad \text{for every } v \in V_*(I) \tag{3.6}$$

are simple; moreover, $\mu = \lambda^4$ is an eigenvalue if and only if $\lambda > 0$ satisfies the equality

$$\cos(2\lambda\pi)\cosh(2\lambda\sigma) - \cos(2\lambda\sigma)\cosh(2\lambda\pi) + \sin(2\lambda\pi)(\sinh(2\lambda\pi) - \sinh(2\lambda\sigma)) + \sinh(2\lambda\pi)(\sin(2\lambda\pi) - \sin(2\lambda\sigma)) =$$

$$4\sin[\lambda(\sigma-\pi)]\sinh[\lambda(\sigma-\pi)].$$

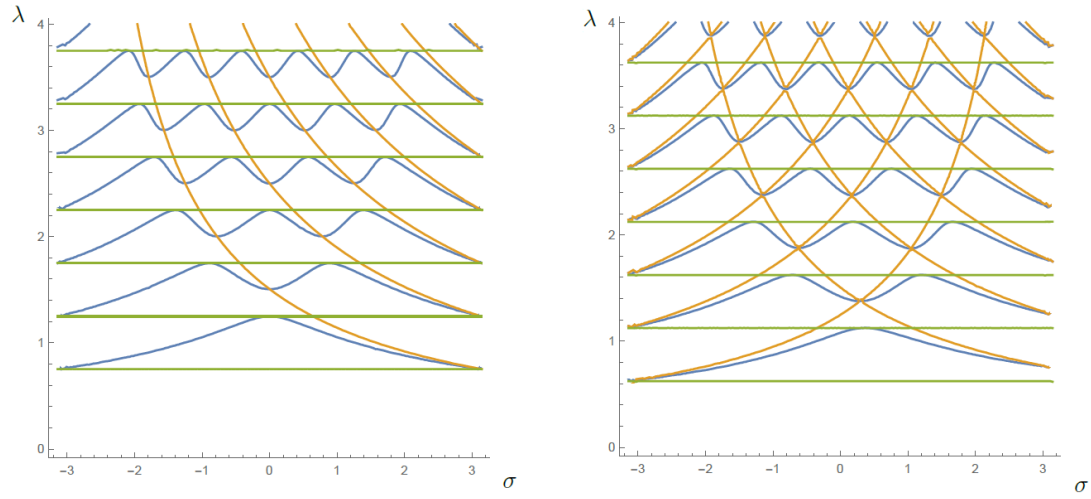

Figure 6. For the clamped problem (left picture) and for the left-clamped and right-hinged problem (right picture), we depict the eigenvalue curves (blue) and the curves implicitly defined by the equations corresponding, respectively, to C^4-eigenfunctions (green) and to eigenfunctions with a double zero in the pier (orange).

In Figure 7, we depict the first twelve eigenfunctions of problem (3.6).

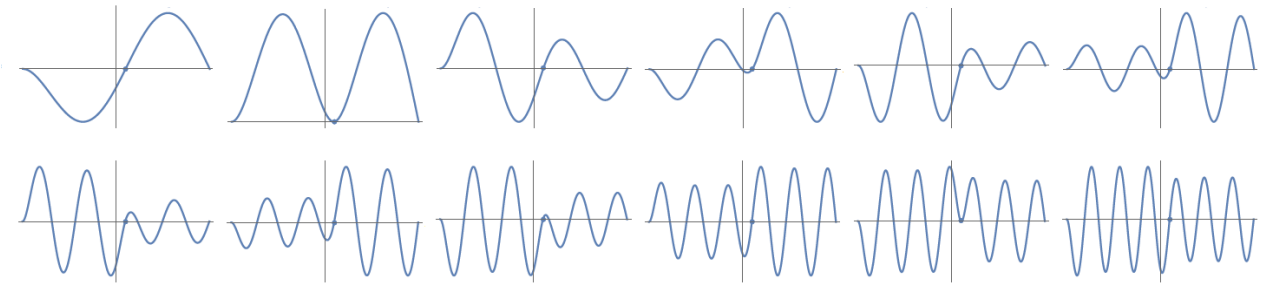

Figure 7. The shape of the first twelve eigenfunctions for the left-clamped and right-hinged problem (3.6) with $\sigma = \pi/10$.

Analogously as before, C^4-eigenfunctions e_λ are possible if and only if

$$\cosh(2\lambda\pi)\cos(\lambda\pi)\sin(\lambda\pi) = \cos(2\lambda\pi)\cosh(\lambda\pi)\sinh(\lambda\pi)$$

while double zeros are possible in correspondence of the pier σ if and only if

$$\cos[\lambda(\pi+\sigma)]\cosh[\lambda(\pi+\sigma)] = 1 \quad \text{and} \quad \sin[\lambda(\pi-\sigma)]\cosh[\lambda(\pi-\sigma)] = \sinh[\lambda(\pi-\sigma)]\cos[\lambda(\pi-\sigma)]. \quad (3.7)$$

The numerical evidence given in the right picture of Figure 6 is in line with the previous discussions and confirms that the criticality principle for C^4-eigenfunctions and for eigenfunctions with a double zero in the pier seems a general fact. Notice that, of course, the picture is here non-symmetric with

respect to $\sigma = 0$, and the general portrait seems to be shifted towards the hinged endpoint; moreover, in order to have a double zero of the corresponding eigenfunction we here need the two conditions in (3.7) (roughly speaking, one for the hinged end and one for the clamped end) which, however, become the same exactly in correspondence of the minima on the eigenvalue curves.

We now observe that, if $\mu = \lambda^4$ and $\mu = \rho^4$ are two different eigenvalues of one of the problems (2.1), (3.3) or (3.6) and u is as in (3.2), w and z satisfy the system

$$\begin{cases} \ddot{w}(t) + \lambda^4 w(t) + (w(t)^2 + z(t)^2)w(t) = 0 \\ \ddot{z}(t) + \rho^4 z(t) + (w(t)^2 + z(t)^2)z(t) = 0. \end{cases} \tag{3.8}$$

Notice indeed that the basis of eigenfunctions obtained by solving problems (2.1), (3.3) or (3.6) is always L^2-orthogonal. System (3.8) is complemented with the initial conditions

$$w(0) = \delta,\ \dot{w}(0) = 0,\ z(0) = z_0 \ll \delta,\ \dot{z}(0) = 0.$$

We are thus making our observation start after that an external force has given an energy input to the system so as to concentrate its oscillations on the component w and we assume, from there on, that the energy dissipation perfectly balances the residual external energy input, so that we can consider an autonomous system. It is the structure that now "manages" the total energy; by "stability" of the system, we intuitively mean that it is not likely that a significant amount of such energy is transferred to the z-component. The way of measuring this significance depends on the considered notion of stability. In terms of linear stability, we observe that if $z_0 = 0$, then (3.8) is satisfied by $(w(t), z(t)) = (W_\lambda(t), 0)$, where W_λ is the (periodic) solution of the Cauchy problem

$$\ddot{W}_\lambda(t) + \lambda^4 W_\lambda(t) + W_\lambda(t)^3 = 0, \quad W_\lambda(0) = \delta, \quad \dot{W}_\lambda(0) = 0,$$

for which an explicit expression is available in terms of the Jacobi functions (notice that the differential equation is of Duffing type). We then linearize (3.8) around $(W_\lambda, 0)$ and we wonder whether $z \equiv 0$ is a stable solution of the obtained equation for the z-variable. More precisely, we give the following definition.

Definition 11. *We say that the "λ-nonlinear mode" W_λ is* linearly stable *(resp.,* unstable*) with respect to the "ρ-nonlinear-mode" if $\xi \equiv 0$ is a stable (resp., unstable) solution of the linear Hill equation*

$$\ddot{\xi}(t) + \left(\rho^4 + W_\lambda(t)^2\right)\xi(t) = 0. \tag{3.9}$$

The analysis of the linear stability for (3.9) was performed in details in [4], so we only report the main results and then interpret them in light of Theorems 1, 9, 10. This is one of the few cases in which the instability regions are completely determined, in dependence on the parameters ρ^4/λ^4 and δ/λ^2; this may be proved using [6] and the results in [8, 9], which ensure that the instability tongues other than the first one are degenerate. Explicitly, the following holds [4, Proposition 3.4].

Proposition 12. *Let $\mu = \lambda^4$ and $\mu = \rho^4$ be two eigenvalues of one of the problems* (2.1)*,* (3.3) *or* (3.6)*, with $\lambda \neq \rho$. Then, the λ-nonlinear-mode of (initial) amplitude δ is linearly stable with respect to the ρ-nonlinear-mode if and only if one of the following facts holds:*

$$\lambda > \rho \text{ and } \delta > 0 \qquad \text{or} \qquad \lambda < \rho \text{ and } \delta \leq \sqrt{2(\rho^4 - \lambda^4)}.$$

This means that once λ and ρ are fixed, the critical amplitude δ from which the system starts becoming linearly unstable is $\bar{\delta} = \sqrt{2(\rho^4 - \lambda^4)}$. Equivalently, the region of instability is described by the inequalities

$$1 < \frac{\rho^4}{\lambda^4} < 1 + \frac{1}{2}\Big(\frac{\delta}{\lambda^2}\Big)^2$$

(see Figure 8).

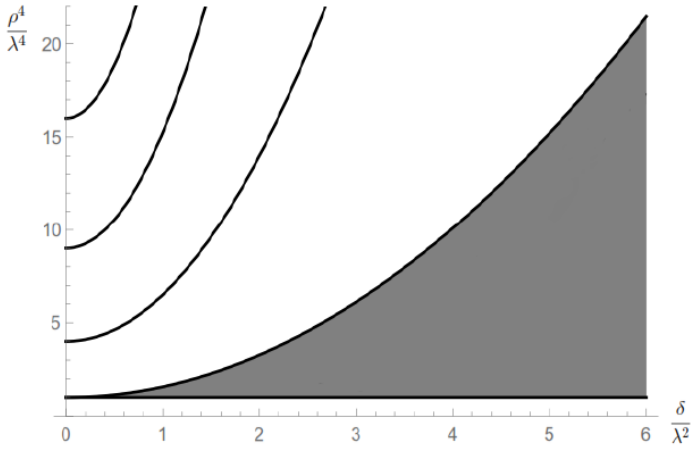

Figure 8. Regions of linear stability (white) and linear instability (gray) for (3.9).

With a couple (λ, ρ), we can then associate a critical energy threshold of instability, given by

$$E(\lambda, \rho) = \frac{\lambda^4}{2}\frac{\bar{\delta}^2}{2} + \frac{1}{4}\frac{\bar{\delta}^4}{4}, \tag{3.10}$$

namely the (preserved) energy of the w-component of the system corresponding to the potential initial configuration of amplitude $\bar{\delta}$. In view of Proposition 12, for the linear instability it is $E(\lambda, \rho) = \rho^4(\rho^4 - \lambda^4)$. The overall energy threshold of instability for the beam $I = [-\pi, \pi]$ with a pier at the point σ is then defined as

$$E(\sigma) = \inf_{k, j \neq k} E(\lambda_k(\sigma), \lambda_j(\sigma)) = \inf_k E(\lambda_k(\sigma), \lambda_{k+1}(\sigma)).$$

This threshold could in principle be equal to 0, also recalling that $\lambda_{k+1}/\lambda_k \to 1$ for $k \to +\infty$; however, usually one truncates the system at a fixed order and reasons only on a finite number of modes, since in practice the dynamics of a real structure is never concentrated on high modes, carrying unrealistically high amounts of energy. We thus set the order of truncation to $N = 12$, as in [3, 4]; with such a position, the above infimum becomes a minimum and, for each σ, the couple (λ, ρ) minimizing the critical energy threshold will be of the kind $(\lambda_k, \lambda_{k+1})$. For each σ, we then numerically determine the energy threshold of instability $E(\sigma)$, for each of the problems (2.1), (3.3) or (3.6), and we represent the obtained results in Figure 9.

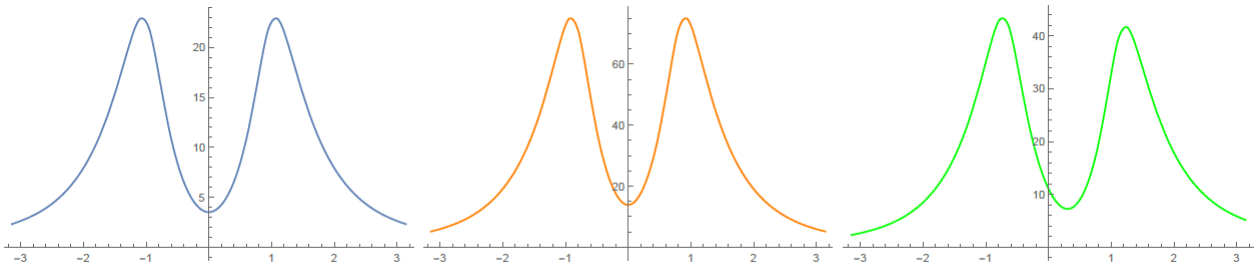

Figure 9. A comparison between the energy thresholds of linear instability for problems (2.1) (left), (3.3) (middle) and (3.6) (right).

We observe the two following facts:

1) a hinged beam is in general less stable than a beam with at least one clamped endpoint;
2) $\sigma = 0$ is a local minimum for E both in the hinged and in the clamped case.

In particular, Item 2) says that, for a beam with a single pier,

the symmetry of the spans weakens the stability of the beam.

This is quite reasonable; the ratio $\lambda_1(\sigma)/\lambda_0(\sigma)$ reaches a local minimum for $\sigma = 0$, since λ_1 has a local minimum at $\sigma = 0$ while λ_0 has a global maximum therein. Hence, at $\sigma = 0$ we approach the lower bound $\rho/\lambda = 1$ of the linear instability region in Figure 8.

The same portrait is displayed when considering instability according to the nonlinear definition given in [3], which we here briefly recall. Roughly speaking, in order to have nonlinear instability a Fourier component which is small at the beginning has to display a *significant* and *abrupt* growth along the considered time interval.

Definition 13. *Let $\eta \in (0,1)$ and $T_W > 0$ be fixed. We say that a weak solution u of* (3.1) *in the form* (3.2) *is unstable before time $T > 2T_W$ if there exists a time instant τ with $2T_W < \tau < T$ such that*

$$(i)\ \|z\|_{L^\infty(0,\tau)} > \eta \|w\|_{L^\infty(0,\tau)} \quad \textit{and} \quad (ii)\ \frac{\|z\|_{L^\infty(0,\tau)}}{\|z\|_{L^\infty(0,\tau/2)}} > \frac{1}{\eta}. \tag{3.11}$$

We say that u is stable until time T if (3.11) *is not fulfilled for any $\tau \in (2T_W, T)$.*

The number $T_W > 0$ plays the role of the so-called *Wagner time*; we refer the reader to the related discussion in [4] about its meaning, which here does not play a central role. Choosing $\eta = 0.1$ and T_W as the period of W_λ (which varies with the initial amplitude $w(0) = \delta$), we have numerically checked such a definition for the hinged, the clamped and the mixed (left clamped-right hinged) problem. We proceeded starting from the left endpoint $-\pi$ and increasing σ with a step of $\pi/20$, spotting nonlinear instability according to the algorithm illustrated in [4, Section 5.5]. In Table 1, we report the energy thresholds of instability found for the hinged case via formula (3.10); the expression therein is computed in correspondence of the least $\bar{\delta}$ for which *nonlinear* instability is found.

Table 1. Energy thresholds of nonlinear instability for hinged boundary conditions.

σ/π	0	0.05	0.1	0.15	0.2	0.25	0.3	0.35	0.4	0.45	0.5	0.55	0.6	0.65	0.7	0.75	0.8	0.85	0.9	0.95	no piers
energy	7.9	8.08	9.95	13.57	17.01	23.99	30.5	31.62	28.49	24.08	19.7	17.33	14.56	11.96	9.89	8.79	8.6	7.62	6.5	5.72	3.88

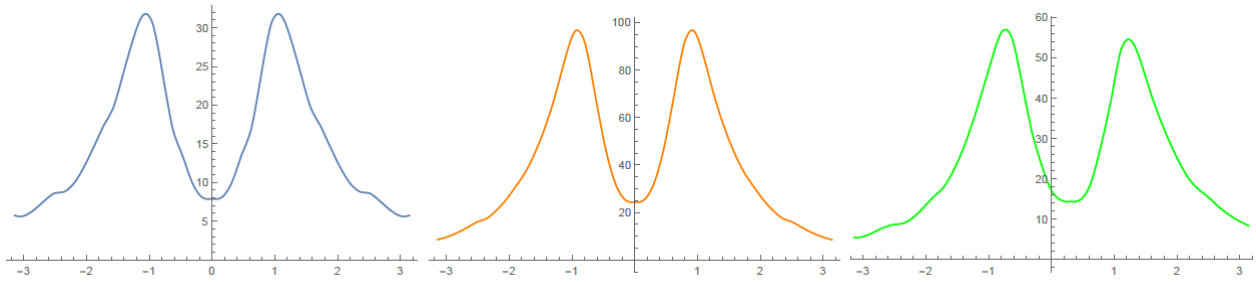

Figure 10. A comparison between the energy thresholds of nonlinear instability for problems (2.1) (left), (3.3) (middle) and (3.6) (right).

By looking carefully at Figure 10, we see that the pictures for linear and nonlinear instability are very similar. In particular, we infer that:

1) for Eq (3.1), linear instability is a clue for the onset of nonlinear instability (as in [4]);
2) the hinged beam appears less stable than a beam with at least a clamped endpoint.

Looking at both the pictures for linear and nonlinear instability, we conclude that, for the considered problems,

the optimal placement of the pier in terms of stability is approximately given by $\sigma = \pm\pi/3$.

Of course, for the mixed problem the asymmetry of the boundary conditions makes only one of these choices of σ the best possible (the closest to the clamped endpoint). In any case, this statement is reminiscent of the picture found for a beam with two symmetric piers [4], where the optimal position of the piers approximately makes the central span twice as long as the lateral spans; indeed, in our setting the choice $\sigma = \pm\pi/3$ divides the beam into two spans having length ratio $2 : 1$. Comparing with [4, Table 3.10], together with Figure 10, we also infer that

1) the presence of at least one pier in general stabilizes the structure with respect to longitudinal energy transfers (compare with the column "No piers" in [4, Table 3.10]);
2) from the point of view of stability, two symmetric piers are in general better than a single pier if the ratio between the lengths of the central and of each lateral span ranges approximately between $6/7$ and $14/3$ (compare the highest energy threshold 31.62 in Table 1 with the ones in [4, Table 3.10]); if instead the two piers are too close either one to the other or to the endpoints, the choice of a single pier is more favourable.

Such conclusions will be the starting point for a future investigation involving models for structures of degenerate plate-type, giving rise to more reliable descriptions of the dynamics of a real bridge.

Acknowledgments

The author acknowledges the support of GNAMPA-INdAM (Gruppo Nazionale per l'Analisi Matematica, la Probabilità e le loro Applicazioni - Istituto Nazionale di Alta Matematica "F. Severi", Rome) and of the PRIN 2017 Project "Direct and inverse problems for partial differential equations: theoretical aspects and applications".

Conflict of interest

The author declares no conflict of interest.

References

1. Burdina VI (1953) Boundedness of solutions of a system of differential equations. *Dokl Akad Nauk SSSR* 92: 603–606.
2. Cazenave T, Weissler FB (1996) Unstable simple modes of the nonlinear string. *Quart Appl Math* 54: 287–305.
3. Garrione M, Gazzola F (2017) Loss of energy concentration in nonlinear evolution beam equations. *J Nonlinear Sci* 27: 1789–1827.
4. Garrione M, Gazzola F (2019) *Nonlinear Equations for Beams and Degenerate Plates with Piers*, Cham: SpringerBriefs in Applied Sciences and Technology, Springer.
5. Garrione M, Gazzola F (2020) Linear theory for beams with intermediate piers. *Commun Contemp Math* DOI: 10.1142/S0219199719500810.
6. Gasparetto C, Gazzola F (2018) Resonance tongues for the Hill equation with Duffing coefficients and instabilities in a nonlinear beam equation. *Commun Contemp Math* 20: 1–22.
7. Gazzola F (2015) *Mathematical Models for Suspension Bridges*, Cham: Springer.
8. Gesztesy F, Weikard R (1996) Picard potentials and Hill's equation on a torus. *Acta Math* 176: 73–107.
9. Goldberg W, Hochstadt H (1996) On a Hill's equation with two gaps in its spectrum. *SIAM J Math Anal* 10: 1069–1076.
10. Harazaki I, Suzuki S, Okukawa A (2000) *Suspension Bridges, Bridge Engineering Handbook*, Boca Raton: CRC Press.
11. Holubová G, Nečesal P (2010) The Fučik spectra for multi-point boundary-value problems. *Electronic H Diff Eq Conf* 18: 33–44.
12. Yakubovich VA, Starzhinskii VM (1975) *Linear Differential Equations with Periodic Coefficients*, New York: J. Wiley & Sons.

AIMS Press